

## Accepted Manuscript

Title: Continuous twin-screw granulation for enhancing the dissolution of poorly water soluble drug

Author: Mohammed Maniruzzaman Arun Nair Maxcene Renault Uttom Nandi Nicholaos Scoutaris Richard Farnish Mike Bradley Martin J. Snowden Dennis Douroumis



PII: S0378-5173(15)30223-4  
DOI: <http://dx.doi.org/doi:10.1016/j.ijpharm.2015.09.025>  
Reference: IJP 15210

To appear in: *International Journal of Pharmaceutics*

Received date: 19-8-2015  
Revised date: 11-9-2015  
Accepted date: 14-9-2015

Please cite this article as: Maniruzzaman, Mohammed, Nair, Arun, Renault, Maxcene, Nandi, Uttom, Scoutaris, Nicholaos, Farnish, Richard, Bradley, Mike, Snowden, Martin J., Douroumis, Dennis, Continuous twin-screw granulation for enhancing the dissolution of poorly water soluble drug. *International Journal of Pharmaceutics* <http://dx.doi.org/10.1016/j.ijpharm.2015.09.025>

This is a PDF file of an unedited manuscript that has been accepted for publication. As a service to our customers we are providing this early version of the manuscript. The manuscript will undergo copyediting, typesetting, and review of the resulting proof before it is published in its final form. Please note that during the production process errors may be discovered which could affect the content, and all legal disclaimers that apply to the journal pertain.

# Continuous twin-screw granulation for enhancing the dissolution of poorly water soluble drug

Mohammed Maniruzzaman<sup>1\*</sup>, Arun Nair<sup>2</sup>, Maxcene Renault<sup>3</sup>, Uttom Nandi<sup>1</sup>,  
Nicholaos Scoutaris<sup>1</sup>, Richard Farnish<sup>4</sup>, Mike Bradley<sup>4</sup>, Martin J. Snowden<sup>1</sup>,  
Dennis Douroumis<sup>1\*</sup>

<sup>1</sup>Faculty of Engineering and Science, School of Science, University of Greenwich, Chatham Maritime, Chatham, Kent ME4 4TB, UK

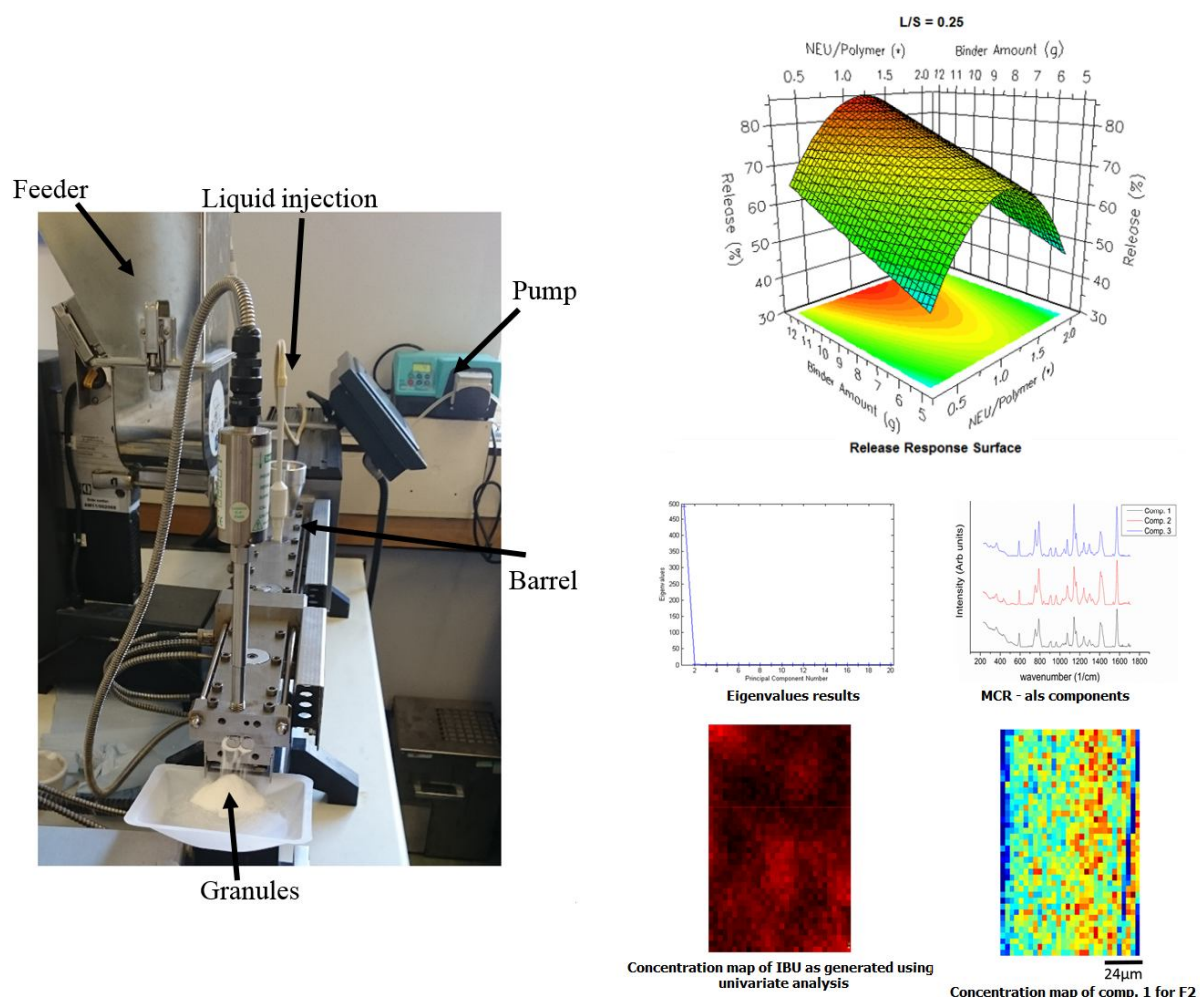
<sup>2</sup>Fuji Chemical Industry Co., Ltd., 12F The Front Tower Shiba Koen, 2-6-3 Shibakoen, Minato-Ward, Tokyo, 105-0011 JAPAN

<sup>3</sup>IUT De Rouen, IUT de Rouen, Bâtiment A - 1er étage, rue Lavoisier, 76821 Mont-Saint-Aignan, CEDEX France

<sup>4</sup>Wolfson Centre of Bulk Solid Handling, Faculty of Engineering and Science, University of Greenwich, Chatham Maritime, Chatham, Kent ME4 4TB

\*To whom correspondence should be addressed: Mohammed Maniruzzaman and Dennis Douroumis, University of Greenwich, Faculty of Engineering and Science, Chatham Maritime, ME4 4TB, Kent, UK, email: [D.Douroumis@gre.ac.uk](mailto:D.Douroumis@gre.ac.uk), [M.Maniruzzaman@gre.ac.uk](mailto:M.Maniruzzaman@gre.ac.uk), Phone: +44 208 331 8440, Fax: 0044 (0) 208 331 9805.

## Graphical abstract



## Abstract

The article describes the application of a twin-screw granulation process to enhance the dissolution rate of the poorly water soluble drug, ibuprofen (IBU). A quality-by-design (QbD) approach was used to manufacture IBU loaded granules via hot-melt extrusion (HME) processing. For the purpose of the study, a design of experiment (DoE) was implemented to assess the effect of the formulation compositions and the processing parameters. This novel approach allowed the use of polymer/inorganic excipients such as hydroxypropyl methylcellulose (HPMC) and magnesium aluminometasilicate (Neusilin®-MAS) with polyethylene glycol 2000 (PEG) as the binder without requiring a further drying step. IBU loaded batches were processed using a twin screw extruder to investigate the effect of **MAS/polymer ratio**, PEG amount (binder) and liquid to solid (L/S) ratios on the dissolution rates, mean particle size and the loss on drying (LoD) of the extruded granules. The

DoE analysis showed that the defined independent variables of the twin screw granulation process have a complex effect on the measured outcomes. The solid state analysis showed the existence of partially amorphous IBU state which had a significant effect on the dissolution enhancement in acidic media. Furthermore, the analysis obtained from the surface mapping by Raman showed the homogenous distribution of the IBU in the extruded granulation formulations.

**Key words:** Granulations, DoE, QbD, dissolutions, twin screw, Raman, DVS.

## 1.0 Introduction

In the recent years, increasing the solubility and thus the bioavailability of poorly water soluble drugs found in oral dosage forms has become a real challenge in pharmaceutical product manufacturing. This has been reflected by the exponential rise in the number of poorly water-soluble drugs in the pharmaceutical pipeline ([Maniruzzaman et al., 2013a](#)). Wet granulation has been adopted as a common process primarily used in the manufacture of pharmaceutical products such as oral solid dosage forms. Historically, the granulation processes have been optimised using conventional high shear and fluidised bed granulation which are suitable for batch manufacturing and are limited by the regulatory issues ([Leuenberger, 2001](#); [Lodaya et al., 2003](#)). Currently twin-screw granulation (TSG) captures a growing interest due to its emerging potential for continuous manufacturing. TSG is easy to scale up for product commercialization with improved manufacturing efficiency

such as reduced production costs and foot print (Cartwright et al., 2013; Keleb et al., 2002; Vervaeet and Remon, 2005). Recently the Food and Drugs Administration (FDA) agency supported the shift from batch mode production to continuous processes which is considered a fundamental step change in the pharmaceutical manufacturing and product development.

Since, the implementation of TSG in mid eighties in the production of paracetamol based extruded granules, this technology has been adopted significantly to primarily focus on its pharmaceutical applications and the process technology (Keleb et al., 2004a,b, 2002; Kleinebudde and Lindner, 1993; Schmidt and Kleinebudde, 1998). A thorough comparison between twin screw granulation techniques and the traditional granulation methods such as high shear granulator (Keleb et al., 2004a; Schmidt and Kleinebudde, 1998) revealed that the twin-screw systems could be used as an alternative continuous manufacturing platform. In a continuous TSG, a higher product yield is achieved by removing the die block at the end of the extruder barrel and thus avoidance of over-compression of the granules is occurred.

Several studies on TSG have significantly explored the influence of process parameters and formulation variables on the critical quality attributes of granulated materials (Dhenge et al., 2013, 2012; El Hagrasy et al., 2013; El Hagrasy and Litster, 2013; Lee et al., 2012; Thompson and Sun, 2010; Tu et al., 2013). Recently Yu et al., (2014), investigated the granulation behaviour of three formulations containing increasing amounts of hydrophobic components using a twin screw granulator. The authors studied the process conditions including powder feed rate, liquid to solid ratio, granulation liquid composition and screw configuration as key parameters to implement a design of experiment (DoE) space. These studies have improved the understanding of the effects of input material properties and processing conditions when optimising a TSG.

Up to date, various studies have been reported on the wet granulations for the formation of the unit dose whereby in-process intermediates of appropriate size, flowability and compressibility are produced prior to downstreaming processes such as tableting. However, the majority of those reported studies have either focused on the compressibility or the process optimisation, but none or very little have reported on the actual effect of this innovative technology on the dissolution rates of poorly water soluble drugs (e.g. ibuprofen). Moreover, the use of inorganic excipients such as magnesium aluminometasilicate (MAS) (Gupta et al., 2002) as drug carriers in TSG for increased dissolution rates of poorly water-soluble drugs can be an attractive approach providing a new insight into translational pharmaceutical research and product development.

MAS is an amorphous magnesium aluminometasilicate with a high specific surface area ( $300 \text{ m}^2/\text{g}$ ) (Gupta et al., 2003) presenting exceptional excipients properties such as high flowability, high surface area, porous, thermal and mechanical stability for improved API delivery and the quality of pharmaceutical dosage forms. Ibuprofen is a BCS class II drug with high permeability and low solubility which has been previously processed via conventional HME for the development of polymeric solid dispersion (Maniruzzaman et al., 2012; 2013a, b). The aim of this article is to exploit the application of TSG to enhance ibuprofen dissolution rates combined with a design of experiment (DoE). The MAS/Polymer ratios, PEG amount as granulating liquid and liquid to solid ratio (L/S) were considered as variables whereas the drug release rate, mean particle size (MPS) and loss on drying (LoD) was measured as response.

## 2. MATERIALS AND METHOD

### 2.1 Materials

Ibuprofen (IBU) was purchased from Tokio Chemical Industries (Belgium) and magnesium aluminometasilicate (MAS-Neusilin® US2) was kindly donated by Fuji Chemical Industries Co., Ltd. (Japan). Hydroxy propyl methyl cellulose based polymer Pharmacoat 603 (HPMC) was kindly donated by ShinEtsu, Japan. Polyethyleneglycole 2000 (PEG) was purchased from Sigma Aldrich (Gillingham, UK). All solvents used were of analytical grade and used as received.

### 2.2 Twin screw granulation and DOE analysis

The granulation experiments were conducted using the twin screw granulator (EuroLab 16, ThermoFisher, Germany) with a screw diameter (D) of 16 mm and barrel length of 40D (L/D ratio 40). The screw configuration used had three kneading zones with same numbers of kneading blocks each. The first kneading zone was configured at  $30^\circ$ ,  $40^\circ$  and  $60^\circ$  angle while the second kneading zone was configured at  $60^\circ$  followed by a third kneading zone just before the die end at  $90^\circ$  angles. During the process, the dry blends of the physical mixtures of the drug, polymer/ inorganic carrier and granulating aid PEG (8-12% w/w ratio) were dispensed into the granulator via a volumetric feeder (Brabender, Germany) at 1 kg/h feed rate. The DoE experiment designs are shown in Table 1. A peristaltic pump enabling the sufficient flow of water as liquid binder was employed to drive the flow of the granulation liquids at a varying flow rate of 4.16-6.67 ml/min for 25-40% (w/w ratio) water

(Fig. 1). The pumps were interfaced with a flow meter to achieve the precise control of the mass flow rate. All extruded granules were further micronized by using a cutter mill (Retsch, Germany) with 250  $\mu\text{m}$  mesh.

Extruded granules with different compositions were obtained by incorporating a threefactorresponse surface fraction factorial design (DoE) inrandomized order by using Fusion One software (DoEFusion One<sup>TM</sup>, USA). Three centrepoint experiments wereperformed as well, resulting in  $2^3+3=11$  experiments. Drug loading was kept constant while MAS/Polymer ratios, granulating liquid concentrations and L/S ratio were considered as variables whereas drug release rate, MPS and LoDwas measuredas dependant variables/response.

### 2.3 Particle size analysis

The particle size distributions of the granules were determined using a Mastersizer 2000 laser diffraction instrument (Malvern Instruments, UK) with a dry powder sample dispersion accessory (Scirocco 2000) and pressure at 2 bar and a vibration feed rate of 50%. Samples were run in triplicate. Mastersizer 2000 software was used for data evaluation. The specific surface area (SSA) of all granules was also measured simultaneously during the particle size analysis by the Mastersizer. The  $d(50)$  reported is the geometric median particle size; the  $d(10)$  and  $d(90)$  are the particle diameters at 10 and 90% of the cumulative volume distribution, respectively. The span of the volume distribution, a measure of the width of the distribution relative to the median diameter, was calculatedusing the following equation (Eq. 1).

$$\text{Span} = \frac{[d_{(90)} - d_{(10)}]}{d_{(50)}} \quad (1)$$

### 2.4 Scanning electron microscopy (SEM)

SEM was used to study the surface morphology of the hot-melt extrudates. The samples were mounted on an aluminium stage using adhesive carbon tape and placed in a low humidity chamber prior to analysis. Samples were coated with gold, and microscopy was performed using a Cambridge Instruments (S630, UK), SEM operating at an accelerating voltage of 5 kV.

### 2.5 X-ray powder diffraction (XRPD)

XRPD was used to determine the solid state of pure active substances, physical mixtures and extruded materials using a Bruker D8 Advance (Germany) in theta-theta mode. For the study purposes a Cu anode at 40kV and 40mA, parallel beam Goebel mirror, 0.2 mm exit slit, LynxEye Position Sensitive Detector with 3° opening (LynxIris at 6.5 mm) and sample rotation at 15 rpm were used. Each sample was scanned from 2 to 40° 2 $\theta$  with a step size of 0.02° 2 $\theta$  and a counting time of 0.1 seconds per step; 176 channels active on the PSD making a total counting time of 35.2 seconds per step

## 2.6 Differential scanning calorimetry (DSC) study

A Mettler-Toledo 823e (Greifensee, Switzerland) differential scanning calorimeter (DSC) was used to carry out DSC runs of pure actives, physical mixtures and extrudates. Approximately 2-5 mg of sample was placed in sealed aluminium pans with pierced lids. The samples were heated at 10°C/min from 0°C to 220°C under dry nitrogen atmosphere and reheated at the same heating rate.

In addition, modulated temperature differential scanning calorimetry (MTDSC) studies were performed from 25°C to 200°C with an underlying heating rate of 2°C/min. The pulse height was adjusted to 2°C with a temperature pulse width of 15-30 s.

## 2.7 Dynamic vapour sorption (DVS) analysis

Vapour sorption of spray-dried powders was investigated by means of an automated gravimetric vapour sorption analyser, DVS Advantage-1 (Surface Measurements Systems Ltd, UK). The DVS Advantage-1 uses a Cahn D200 recording ultramicrobalance with a mass resolution of  $\pm 0.1$   $\mu$ g; the vapour partial pressure around the sample is controlled by mixing saturated and dry carrier gas streams (N<sub>2</sub>) using electronic mass flow controllers (Amaro et al., 2015). Samples were equilibrated at 0% RH until dry and the reference mass was recorded. The samples were exposed to the following relative humidity (% RH) profile: 0 to 90% in 10% steps and the reverse for desorption at 25.0 $\pm$ 0.1°C. At each stage, the sample mass was allowed to reach equilibrium, defined as  $dm/dt=0.002$  mg/min over 10 min, before the RH was changed. The amount of water uptake for each RH stage was expressed as a % of the dry sample mass ( $m_0$ ).

## 2.8 Raman mapping to study the drug distribution

Room temperature Raman spectra of the “pure” formulation components were obtained using a Jobin/Yvon LabRam 320 instrument equipped with an Olympus microscope (Horiba, Japan). The spectrometer is equipped with a 1800 grooves/mm holographic grating,



a holographic notch filter, a Peltier-cooled CCD (MPP1 chip) for detection, and an Olympus BX40 microscope. An Ar<sup>+</sup> ion laser ( $\lambda = 532.8$  nm) was used. Raman spectra of solid-state samples were collected at room temperature on a microscope slide using a microscope objective of 50 $\times$  magnification to focus the laser beam. A backscattering (180 $^\circ$  between excitation and collection) geometry was used in all experiments. Each spectral scan was collected for 5 s using 4 accumulations. The Raman instrument was calibrated using the v1 line of silicon at 520.7  $\text{cm}^{-1}$ . Centering of the silicon line was checked by using the frequencies of the principal lines of a neon lamp.

Raman mapping (Lee et al., 2011; Islam et al., 2015) was performed using a Jobin/Yvon LabRam 320 instrument equipped with an Olympus microscope (Horiba, Japan) by means of Ar<sup>+</sup> ion laser ( $\lambda = 532.8$  nm) and 1800 l/nm grating on 3 different particles for each formulation (Supp. Fig. 1). The experimental conditions were: 100 nm slit width, a 50 $\times$  Microsoft objective and 0.4 s acquisition time. Each spectrum was the mean of the two. The sample profiling was performed at step increments of 3  $\mu\text{m}$  in the X–Y direction covering the biggest possible surface of the part.

In order to investigate the distribution of IBU in the formulations univariate analysis has been applied by using its characteristic peak at 1609  $\text{cm}^{-1}$ . The data analysis were principal component analysis (PCA) as a precursor method to identify the number of component. Subsequently, multivariate curve resolution – alternate least square (MCR - ALS) was used to decompose the hyperspectral data matrix. Prior to analysis, the spectra were baseline by using the automatic weighted least square and normalised to unit area to avoid deviation among the Raman spectra.

## 2.9 *In vitro* dissolution study

*In vitro* drug release studies were carried out in 900 ml of both 0.1 M HCl (pH 1.2) and 0.2 M dihydrogen-sodium-orthophosphate (pH adjusted with NaOH to 6.8) for 2 hr using a Varian 705 DS dissolution paddle apparatus (Varian Inc. North Carolina, US) at 100 rpm. Dissolution bath and vessels were then equilibrated to  $37 \pm 0.5^\circ\text{C}$ . At predetermined time intervals, samples were withdrawn for HPLC assay. All dissolution studies were performed in triplicate.

## 2.10 HPLC analysis

The release of IBU was determined by using HPLC, Agilent Technologies system 1200 series. A HYCHROME S50DS2-4889 (5  $\mu\text{m}$  x 150 mm x 4mm) column was used for the HPLC analysis of IBU. The wavelength was set at 214 nm. The mobile phase consisted of acetonitrile/water/phosphoric acid (65/35/0.2 v/v) and the flow rate was maintained at 1.5 ml/min and the retention time was 2-3 min (Gryckze et al., 2011; US Pharmacopeia, 2015). Calibration curve was prepared with concentrations varying from 10  $\mu\text{g}$  /ml to 50  $\mu\text{g}$ /ml and 20  $\mu\text{l}$  injection volumes.

### 3. RESULTS AND DISCUSSION

#### 3.1 DOE analysis of extrusion granulation

The main objective of this study was not only to manufacture extruded granules processed via continuous twin-screw granulation but also to investigate the effect of various processing parameters/ conditions to identify and define the design space. For the purpose of the study a DoE was implanted to investigate the effect of process variables (independent) such as the MAS/Polymer ratio (A), the binder amount (B) and the liquid/solid (C) ratio on the granulation process. The drug dissolution rate, the mean particle size (MPS) and the loss of drying (LoD) were selected as the dependent variables. The relationship and the effect of the three inputs on all of the targeted response were investigated further. The drug concentration in all formulations was kept constant at 40% (w/w ratios) by keeping the final dosage of IBU (200 mg) in account. The processing conditions such as screw speed, screw configurations and feed rate were also kept steady in order to reduce experiments and the number of processing parameters.

The experimental plan with the discrete values of the independent variables and the measured values of the dependent variables are depicted in Supp. Table 1a. The regression analysis of the DoE revealed interesting results for the extrusion granulation process. As it can be seen from Supp. Table 1b there is a quadratic effect of the MAS/Polymer factor ( $p = 0.01$ ) and no significant effect of the other main process variables on the drug release rates ( $p > 0.05$ ). Interestingly, a two – way interaction of the binder amount and the L/S ratio has a significant effect on the drug release. The most complex effect appeared on the LOD where both binder amount (linear) and L/S (quadratic) were found to present a significant effect ( $p < 0.05$ ). Interestingly, two – way interactions of the A/B and B/C appeared to have a significant effect on the LOD. These two – way interactions indicate a synergetic effect for each of the variable pairs. Finally, the obtained granules particle size is affected significantly (Supp. Table 1c) by the MAS/Polymer ratio and the two – way interaction between the

MAS/Polymer ratio and the binder amount. The DoE analysis shows that the defined independent variables of the extrusion granulation process have a complex effect on the measured outcomes. Thus, further process optimization will require the implementation of an advanced DoE such as a response surface design. The response surface maps for each dependent variable are depicted in Fig. 2.

### 3.2 Particle morphology

SEM was used to examine the surface morphology of the bulk IBU and the extruded granules. As can be seen in Fig. 3(a), bulk IBU appeared as needle type crystals falling in the micro range. In contrast, for all IBU extruded granules, no drug crystals were observed on the granulated surface suggesting excellent mixing during the high shear granulation (torque ~3.6 – 5.2 Nm, engine load ~0.05-0.10 KW) inside the extruder barrel. This may result in a possible drug adsorption into the porous MAS network in room temperature for the granulated formulations (Fig. 3b-d). Further information provided in supplementary data (Supp. Fig. 2). It can also be seen that all IBU loaded granules appeared as agglomerates of microstructured particles. This formation of such extruded granules with drug adsorption and reduced granular particle size during extrusion can be of great interest for the development of oral dosage forms with enhanced dissolution rates of poorly water-soluble drugs.

Particle size volume distributions for all extruded granules were either monomodal or dimodal with low span values (1.5 to 13.3) (Supp. Fig. 3). The geometric median particle size (d<sub>50</sub>) for all IBU extruded granules was in the range of 100–305 μm and the SSA was 0.04–0.92 m<sup>2</sup>/g. The d<sub>50</sub> values of all extruded granules are summarized in Table 1 (and Supp. Table 1c) and affected mainly by the MAS/Polymer amounts and the two way interaction with the binder amounts. Furthermore the response surface maps (Fig. 2) shows that granule particle sizes (~100 - 110 μm) are obtained for MAS/Polymer ratios close to 1 while binder amounts vary from 5-8%. For any other MAS/Polymer ratio the granule particle size increases up to 305 μm. The DOE regression analysis also revealed that the L/S ratio did not present any effect on the granule size which was in a good agreement with previous studies (Dhenge et al. 2012).

The LoD values of the extruded granules are not affected by the MAS/Polymer ratios but are heavily depend on the binder amounts and the L/S ratios. The contour map (Supp. Fig. 4) shows that low LoDs can be achieved for low L/S ratios (0.25 – 0.30) and high binder concentrations (8 – 12%). The manufacturing of granules with low LoD is very important for

the development of solid dosage forms such as tablets in order to avoid powder sticking on the tablet press punches or capping and lamination of the compressed tablets in a later stage.

A novel aspect of the implemented granulation process is the fact that excellent granules with optimised particle size distribution and low LoD values can be obtained without using an additional drying step. The granule drying is a critical step in continuous granulations. This was attributed to the unique combination of inorganic and polymer excipients

### 3.3 X-ray powder diffraction (XRPD)

X-ray analysis of bulk substances and the IBU/MAS/HPMC/PEG granules, was conducted in order to examine the crystalline state of the drug. As can be seen in Fig. 4, the diffractogram of pure IBU presented distinct intensity peaks due to its crystalline structure at  $6.03^\circ$ ,  $12.09^\circ$ ,  $16.48^\circ$ ,  $17.55^\circ$ ,  $18.75^\circ$ ,  $20.02^\circ$ ,  $22.13^\circ$ ,  $24.47^\circ$ ,  $24.99^\circ$   $2\theta$  degrees while PEG exhibited two characteristic intensity peaks at  $19.01^\circ$  and  $23.49^\circ$   $2\theta$  degrees. In contrast both MAS and HPMC appeared as completely amorphous (no crystalline intensity peaks). The extruded granules of all IBU formulations showed identical peaks due to the presence of crystalline IBU in the formulations at relatively lower intensities suggesting that the amorphicity of the highly crystalline drug has been increased during the high shear granulation processing even at high 40% drug loading (% w/w).

### 3.4 DSC analysis

DSC was used to determine the solid state of the drug in the extruded granules. Supp. Fig. 5a represents the thermal transitions of pure IBU, PEG and MAS. The bulk IBU showed an endothermic thermal transition at  $77.79^\circ\text{C}$  ( $\Delta H = 92.99 \text{ j/g}$ ), which corresponds to its melting peak while PEG exhibited an endothermic sharp melting peak at  $52.82^\circ\text{C}$  ( $\Delta H = 133.39^\circ\text{C}$ ). In contrast, the bulk HPMC did not show any transitions due to its amorphous nature. Similarly, the MAS did not present any endothermic thermal event suggesting that the inorganic MAS is amorphous with relatively higher glass transitions. The DSC analysis (Fig. 5 and Supp. Fig. 5b) of the physical blends of all formulations showed an endothermic thermal transition at about  $53\text{-}54^\circ\text{C}$  corresponding to the melting of crystalline PEG followed by another thermal event at about  $77^\circ\text{C}$  corresponding to the melting of IBU present in the formulations. Similarly, the DSC thermograms of extruded granules showed the melting peaks of IBU at relatively lower temperature attributed to the amorphicity increase of the IBU in the extruded granules as complemented by XRD analysis above. This could also be for the

partial solubilisation of the drugs in low melting point PEG and entrapment in the porous network of inorganic MAS. The thermal transition due to the melting of IBU in the extruded formulations were visible at 61.79-67.29°C just after the melting transitions of the crystalline PEG.

### 3.5 DVS analysis

The effect of moisture on the solid-state stability of the drug in different granules prepared via the continuous twin screw granulation processing was investigated by DVS. It was expected that the inclusion of hydrophilic HPMC and PEG along with MAS would lead to an increase in the water uptake capacity of the extruded granules. The presence of MAS in the formulations will ease the water uptake as it works as an excellent proton donor and receptor due to the presence of sialols in its structure. Fig. 6 shows the water vapour sorption isotherms for three different extruded granules. F2 took up approximately 3.73% by mass at 60% RH (25°C and 40°C temperature) followed by a significant increase of up to 13.20% by mass of moisture at 100% RH. The desorption isotherm shows steady water loss, resulting in a reversible process. Similar vapour sorption isotherms were seen for F10 where about 9.88% by mass at 100% RH was increased in the absorption segment at both 25°C and 40°C suggesting that the vapour sorption was not dependant on the temperature but the RH %. In contrary, F11 showed an interesting event in both the sorption and the desorption segment. Unlike at 40°C, it took up a very little mass of moisture at 25°C with no further water loss or gain in the desorption isotherm represented by a steady line at 25°C, resulting in an open hysteresis (Tewes et al., 2010). These events are believed to occur as a result of partial amorphous IBU collapsing into its crystalline stable form, as crystalline phases are less hydrophilic than amorphous ones. Similar studies were reported elsewhere (Amaro et al., 2015). Excessive amount of PEG (12% w/w) present in the formulation F11 may have played a vital role for this event while F2 and F10 both have lesser amount in the formulations. It can also be seen from DVS analysis that up to 30% of water as a granulating liquid could prove to be optimum for developing stable granules for dissolution enhancement purpose via twin-screw granulations.

### 3.6 Confocal Raman mapping

The Raman spectra of the pure compounds are represented in Supp. Fig. 6. As it can be observed, IBU has a characteristic peak at 1609  $\text{cm}^{-1}$  which has been used to investigate the distribution of the drug in the formulation by means of univariate analysis. Fig. 7(a-c) demonstrates the distribution of IBU in all the particle area. However, in F1 IBU is not

evenly dispersed as there is an area (bottom right corner) with higher concentration (Fig. 7a). Additionally, in order to investigate the homogeneity of the formulation multivariate data analysis has been used. Specifically, PCA was applied as a precursor to MCR to reduce the number of variables and identify the number of components. In general, the decision of when to stop extracting principal components basically depends on when there is only very little "random" variability left. The nature of this decision is arbitrary; however, various guidelines have been developed. One of the most common approach used in Raman mapping is Kaiser Criterion where the PCs that are retained have eigenvalues more than F1. Based on this criterion, it is clear that in F2 and F6 the system can be described by using only one component which contains peaks from all the compounds indicating the homogeneity of the samples where F1 will use four components to decompose the hyperspectral data matrix. It is worth noting that the graphs of eigenvalues have already suggested that the F2 and F6 are more homogenous than F1.

In terms of F1, the hyperspectral data matrix was decomposed in four components. Fig. 6b represents some characteristic bands of the compounds that appear in the first four components after MCR decomposition. Hence, as it can be seen components 1 and 2 contain peaks attributed to IBU and PEG only, whereas characteristic peaks of MAS and HPMC appeared in the 4<sup>th</sup> components at 587cm<sup>-1</sup> and 290cm<sup>-1</sup> respectively. Other bands are possible to appear but they were not able to distinguish as they are overlapped with the strong IBU peak. Finally, Fig. 7a also illustrates the areas that correspond to the components 1, 2 and 4 where it can be seen that HPMC has not covered the whole area. This has also been confirmed by applying Classical Least Square method (CLS) (data are not represented). It is worth mentioning that the main reason of this non-homogenous distribution is the appearance of amorphous and crystalline drug. In crystalline IBU the peaks in the region 780 – 835 cm<sup>-1</sup> are more acute as in the case of component 1, whereas the amorphous drug gives broader peak in this region similar to component 4 (Hédoux et al., 2011). Consequently, HPMC may inhibit drug's crystallisation as these two compounds co-exist in the same face.

In terms of F2 and F6, the data matrix was decomposed in three components (Fig. 7b-c). As it can be seen, these components are similar and contain peaks related to all the compounds confirming the homogeneity of these formulations. Moreover, the IBU in these formulations are in partially amorphous state leading to a more uniform formulation.

### **3.7 *In vitro* dissolution studies**

The main aim of the study was to manufacture granulated formulations to impact on the dissolution profiles of hydrophobic drug IBU. In Fig. 8, it can be seen that the manufactured granules with high drug loading 40% (w/w ratios) showed significant increase in the dissolution rate of IBU varying from 60-85% within 120 min complying with the USP monograph ([US Pharmacopeia, 2015](#)). Additional results are provided in Supp. Fig. 7a. As mentioned previously regression analysis showed significant effect of the MAS/Polymer ratio and a two-way interaction of the B/C factors on the release patterns. As shown in the contour map of Supp. Fig. 7b, high IBU release rates can be obtained for equal MAS/Polymer amounts (1:1 ratio), high binder amounts (> 8%) and low L/S ratios (<0.3). Thus F2, F10 and F11 showed the high IBU release rates with the latter being the optimal formulation for the extrusion granulation processing. This particular formulation outperformed the rest compositions due to the appropriate MAS/Polymer ratio (1:1) and the synergetic effect of the high binder amount (12%) and low L/S ratio (0.25). As a result F11 presented the high dissolution rates, narrow particle size distribution and low LoD value.

#### **4.0 Conclusions**

A twin screw continuous granulation process was used to manufacture IBU loaded fast-release granules by investigating the effect of MAS/Polymer ratio, PEG concentration, and L/S ratio on the dependant variables such as release, mean particle size and LoD. By implementing a DoE approach, it was revealed that the defined independent variables of the twin screw granulation process have a complex effect on the measured outcomes. The solid state analysis showed the existence of the IBU in its partially amorphous forms which may have significant effect on the dissolution enhancement. Furthermore, the analysis obtained from the surface mapping by Raman showed the homogenous distribution of the IBU granules in the granulated formulations. An important aspect of the granulation process was the absence of a further drying step and the optimization of granules with the optimum specifications. This promising paradigm of QbD approach can be used in the future for process optimization and better understanding of the developed pharmaceutical formulations via twin-screw granulation.

#### **Acknowledgements**

The authors would like to thank Fuji Chemical Industry Co., Ltd., Japan for the financial contribution.

## 5.0 References

- Amaro, M.I., Tajber, L., Corrigan, O.I., Healy, A.M., 2015. Co-Spray Dried Carbohydrate Microparticles: Crystallisation Delay/Inhibition and Improved Aerosolization Characteristics Through the Incorporation of Hydroxypropyl- $\beta$ -cyclodextrin with Amorphous Raffinose or Trehalose. *Pharm. Res.* 32, 180–195.
- Cartwright, J.J., Robertson, J., D'Haene, D., Burke, M.D., Hennenkamp, J.R., 2013. Twin screw wet granulation: loss in weight feeding of a poorly flowing active pharmaceutical ingredient. *Powder Technol.* 238, 116–121.
- Dhenge, R.M., Cartwright, J.J., Houslow, M.J., Salman, A.D., 2012. Twin screw wet granulation: effect of properties of granulation liquid. *Powder Technol.* 229, 126–136.
- Dhenge, R.M., Washino, K., Cartwright, J.J., Houslow, M.J., Salman, A.D., 2013. Twin screw granulation using conveying screws: effect of viscosity of granulation liquids and flow of powders. *Powder Technol.* 238, 77–90.
- El Hagrasy, A.S., Hennenkamp, J.R., Burke, M.D., Cartwright, J.J., Litster, J.D., 2013. Twin screw wet granulation: influence of formulation parameters on granule properties and growth behaviour. *Powder Technol.* 238, 108–115.
- El Hagrasy, A.S., Litster, J.D., 2013. Granulation rate processes in the kneading elements of a twin screw granulator. *AIChE J.* 59, 4100–4115.
- Gryczke, A., Schminke, G.S., Maniruzzaman, M., Beck, J., Douroumis, D., 2011. Development and evaluation of orally disintegrating tablets (ODTs) containing ibuprofen granules prepared by hot melt extrusion. *Colloids Surf B Biointerfaces* 86, 275-84.
- Gupta, M.K., Tseng, Y-C., Goldman, D., Bogner, R.H., 2002. Hydrogen Bonding with Adsorbent during Storage Governs Drug Dissolution from Solid-Dispersion Granules. *Pharm Res* 19, 1663-72.
- Gupta, M.K., Vanwert, V., Bogner, R.H., 2003. Formation of Physically Stable Amorphous Drugs by Milling with Neusilin. *J Pharm Sci* 92, 536-51.
- Hédoux, A., Guinet, Y., Derollez, P., Dudognon, E., Correia, N.T., 2011. Raman spectroscopy of racemic ibuprofen: Evidence of molecular disorder in phase II. *International Journal of Pharmaceutics* 421, 45-52.



Islam, M. T., Scoutaris, N., Maniruzzaman, M., Moradiya, H.G., Halsey, S.A., Bradley, M., Chowdhry, B.Z., Snowden, M.J., Douroumis, D., 2015. Implementation of transmission NIR as a PAT tool for monitoring drug transformation during HME processing. *Eur. J. Pharm. Biopharm.* 96, 106–116.

Keleb, E.I., Vermeire, A., Vervaet, C., Remon, J.P., 2002. Continuous twin screw extrusion for the wet granulation of lactose. *Int. J. Pharm.* 239, 69–80.

Keleb, E.I., Vermeire, A., Vervaet, C., Remon, J.P., 2004a. Single-step granulation/ tableting of different grades of lactose: a comparison with higher shear granulation and compression. *Eur. J. Pharm. Biopharm.* 58, 77–82.

Keleb, E.I., Vermeire, A., Vervaet, C., Remon, J.P., 2004b. Twin screw granulation as a simple and efficient tool for continuous wet granulation. *Int. J. Pharm.* 273, 183–194.

Kleinebudde, P., Lindner, H., 1993. Experiments with an instrumented twin-screw extruder using a single-step granulation/extrusion process. *Int. J. Pharm.* 94, 49–58.

Lee, K.T., Ingram, A., Rown, N.A., 2012. Twin screw wet granulation: the study of a continuous twin screw granulator using Positron Emission Particle Tracking (PEPT) technique. *Eur. J. Pharm. Biopharm.* 81, 666–673.

Lee, W. L., Loei, C., Widjaja, E., Loo, S.C.J., 2011. Altering the drug release profiles of double-layered ternary-phase microparticles. *J. Control. Rel.* 151, 229–238.

Leuenberger, H., 2001. New trends in the production of pharmaceutical granules: batch versus continuous processing. *Eur. J. Pharm. Biopharm.* 52, 289–296.

Lodaya, M., Mollan, M., Ghebre-Sellasie, I., 2003. Twin screw granulation. In: Ghebre-Sellasie, I., Martin, C. (Eds.), *Pharmaceutical Extrusion Technology*. Marcel Dekker, New York, pp. 69–98.

Maniruzzaman, M., Boateng, J. S., Snowden, M.J., Douroumis, D., 2012. A review of hot-melt extrusion: process technology to pharmaceutical products. *ISRN Pharmaceutics* 2012, 436763.

Maniruzzaman, M., Morgan, D.J., Mendham, A.P., Pang, J., Snowden, M.J., Douroumis, D., 2013b. Drug-copolymer intermolecular interactions in hot-melt extruded solid dispersions. *Int J Pharm* 443(1-2), 199-208.

Maniruzzaman, M., Rana, M.M., Boateng, J.S, Mitchell, J.C., Douroumis, D., 2013a. Dissolution enhancement of poorly water-soluble APIs processed by hot-melt extrusion using hydrophilic polymers. *Drug Dev Ind Pharm* 39, 218-27.

Schmidt, C., Kleinebudde, P., 1998. Comparison between a twin-screw extruder and a rotary ring die press. Part II: influence of process variables. *Eur. J. Pharm. Biopharm.* 45, 173–179.

Tewes, F., Tajber, L., Corrigan, O.I., Ehrhardt, C., Healy, A.M., 2010. Development and characterisation of soluble polymeric particles for pulmonary peptide delivery. *Eur. J Pharm. Sci.* 41, 337–52.

Thompson, M.R., Sun, J., 2010. Wet granulation in a twin-screw extruder: implications of screw design. *J. Pharm. Sci.* 99, 2090–2103.

Tu, W.D., Ingram, A., Seville, J.P.K., 2013. Regime map development for continuous twin screw granulation. *Chem. Eng. Sci.* 87, 315–326.

US Pharmacopeia ([http://www.usp.org/sites/default/files/usp\\_pdf/EN/USPNF/errata467Ibuprofen.pdf](http://www.usp.org/sites/default/files/usp_pdf/EN/USPNF/errata467Ibuprofen.pdf)), last accessed on Aug 2015.

Vervaeet, C., Remon, J.P., 2005. Continuous granulation in the pharmaceutical industry. *Chem. Eng. Sci.* 60, 3949–3957.

Yu, S., Reynolds, G.K., Huang, Z., Matas, M.D., Salman, A.D., 2014. Granulation of increasingly hydrophobic formulations using a twin screw granulator. *Int. J. Pharm.* 475, 82–96.

## **TABLES**

**Table 1:** Experimental design of continuous granulation formulations with MAS/Polymer ratio, binder amount (%) and L/S ratio as independent variables and Release (%), particle size D(0, 5), and LoD (%) as dependent variables.

Run No.	Process independent variables			Process dependent variables		
	MAS/Polymer ratio	Binder (%)	L/S ratio	Release (%) T <sub>2h</sub>	D(50) ( $\mu\text{m}$ )	LoD (%)
<b>F1</b>	2.0	8.0	0.25	61.89	150	1.82
<b>F2</b>	1.0	8.0	0.30	75.61	100	1.88
<b>F3</b>	0.33	8.0	0.30	48.76	152	2.14
<b>F4</b>	2.0	5.0	0.40	47.26	305	2.37
<b>F5</b>	2.0	12.0	0.30	50.01	170	2.22
<b>F6</b>	1.0	8.0	0.40	61.35	106	1.82
<b>F7</b>	0.33	12.0	0.40	37.61	245	2.84
<b>F8</b>	0.33	5.0	0.25	42.19	124	4.05
<b>F9</b>	1.0	5.0	0.30	50.79	109	3.29
<b>F10</b>	1.0	8.0	0.30	84.02	136	2.15
<b>F11</b>	1.0	12.0	0.25	86.50	124	1.26

### Figures caption list

**Fig** Instrumentation set up for twin-screw granulation comprising of a Eurolab 16 extruder and the  
. 1 granulating liquid feeding pump.

**Fig** Response surface for IBU release and mean particle size in the DoE design space.  
. 2

**Fig** SEM images of (a) bulk IBU, (b) F1, (c) F2 and (d) F6 extruded granules.  
. 3

**Fig** XRPD diffractograms of pure substances and various extruded granules.

. 4

**Fig** DSC thermograms of extruded granules.

. 5

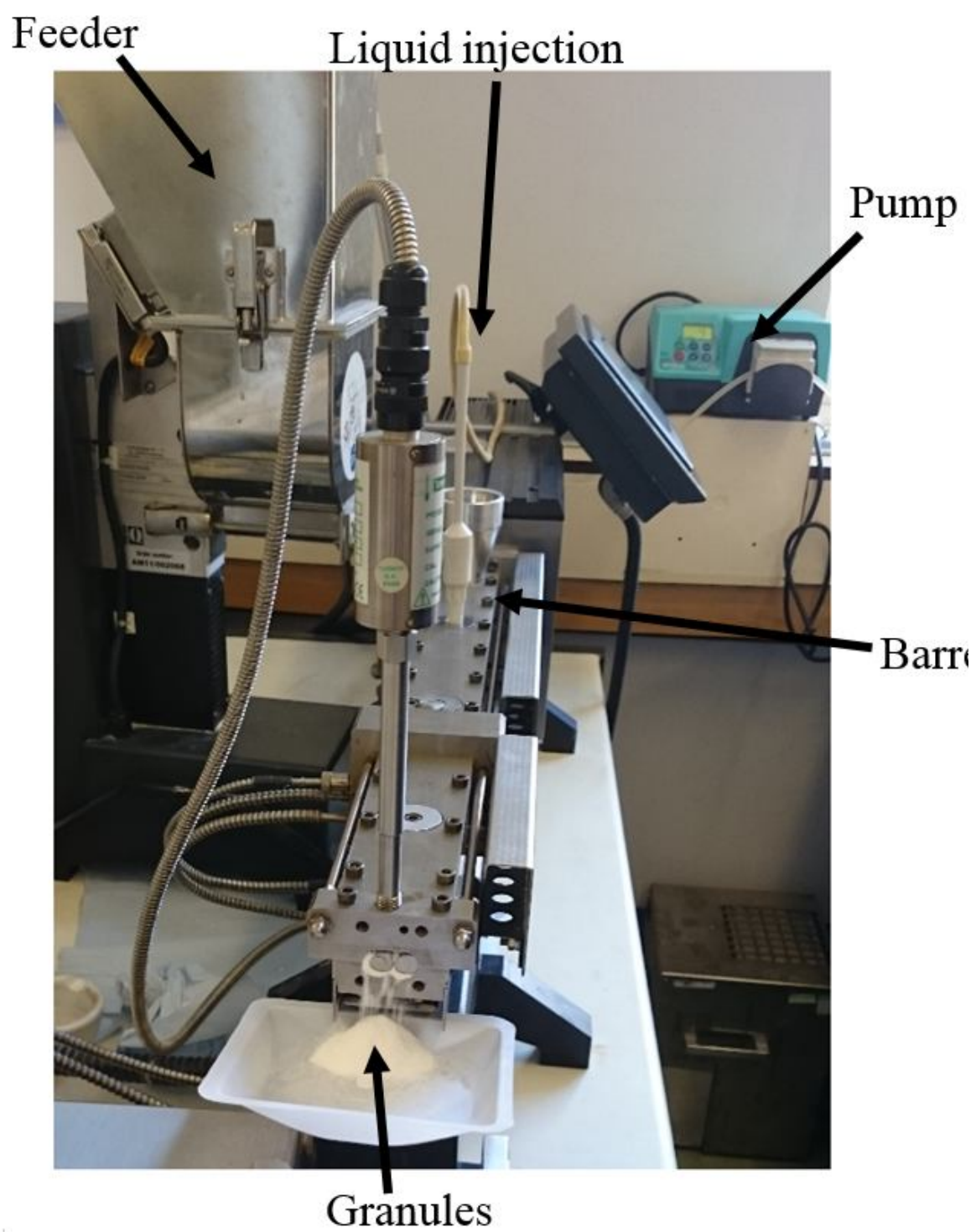
**Fig** DVS analysis of water sorption and desorption of F1, F2 and F6 granules.

. 6

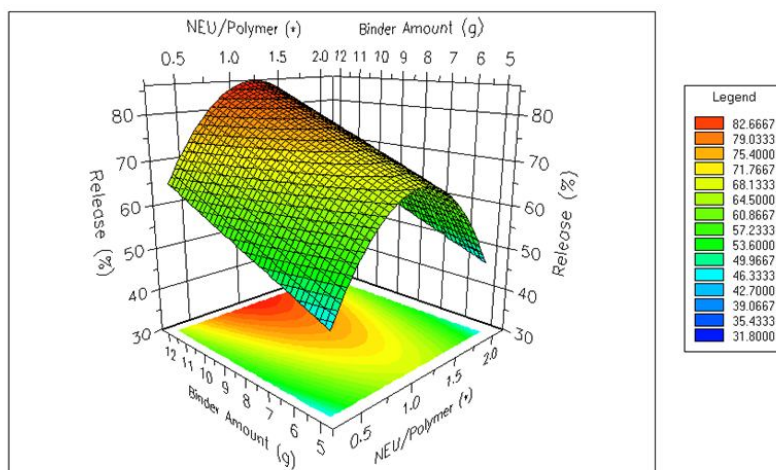
**Fig** (a), (b) and (c) eigenvalues results (top left), MCR –also components where \* represent peaks of IBU, \$ represents peaks of PEG, # peak of HPMC and & peak of MAS (top right), concentration map of IBU as generated using univariate analysis (bottom left) and concentration map of comp. 1 (black), comp 2 (red) and comp 4 (green, bottom right) for F1, F2 and F6, respectively.

**Fig** *In vitro* dissolution studies of IBU from the extruded granules in F2, F10 and F11 (n=3, 37°C, 100 rpm).

. 8

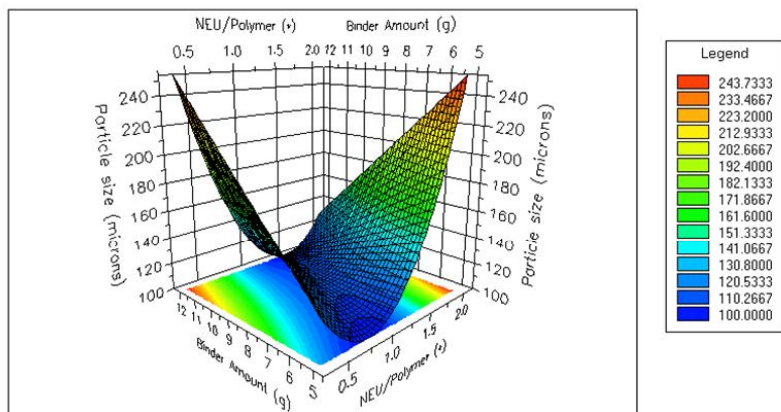


Release Response Surface  
L/S = 0.25



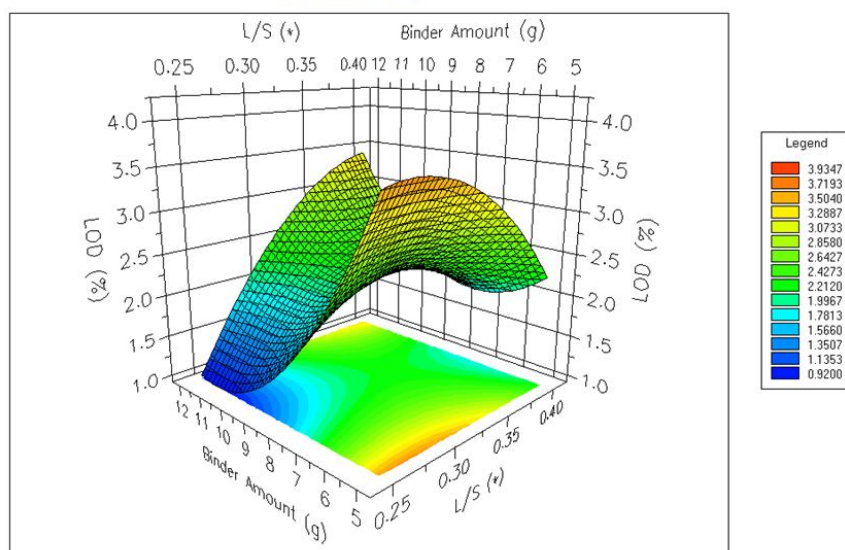
(a)

Particle size Response Surface  
L/S = 0.25

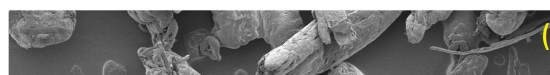
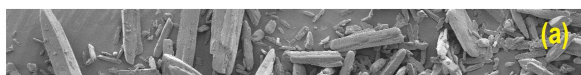


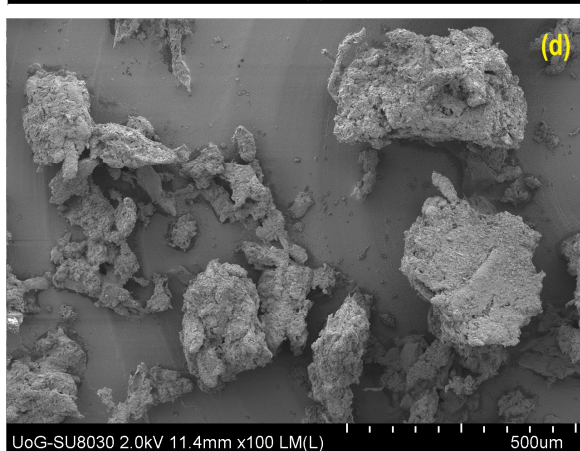
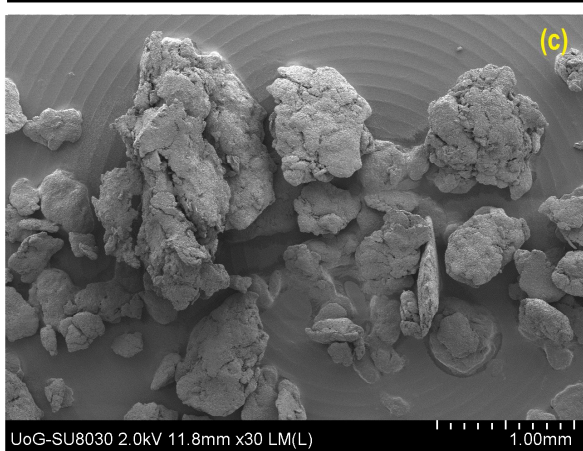
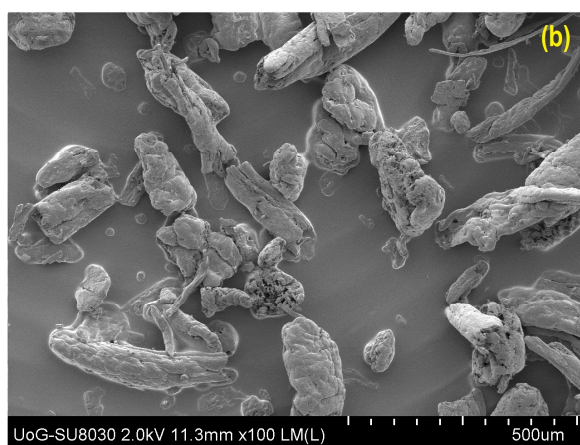
(b)

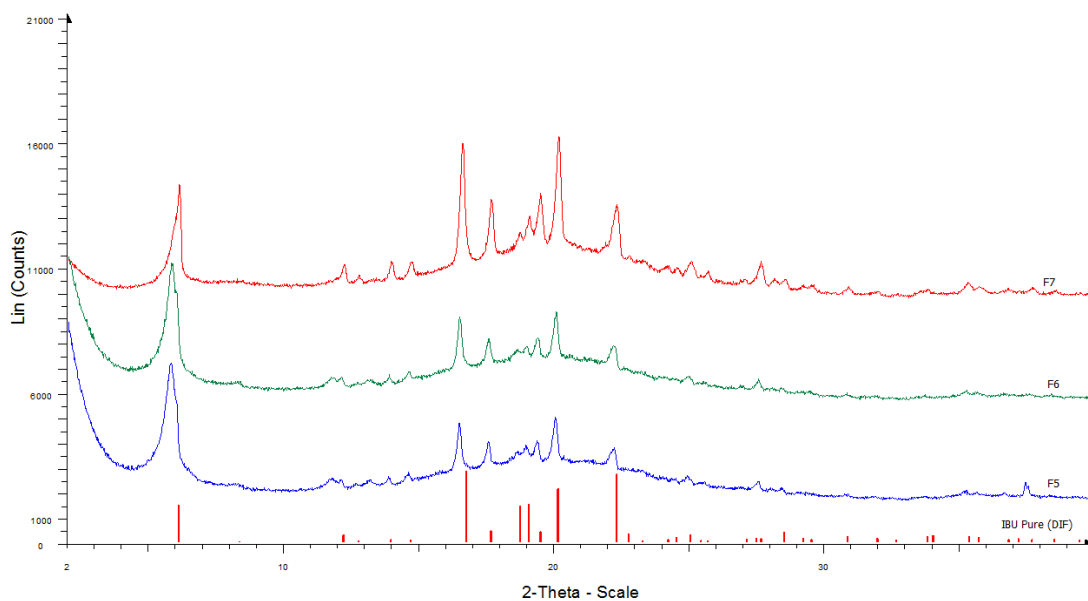
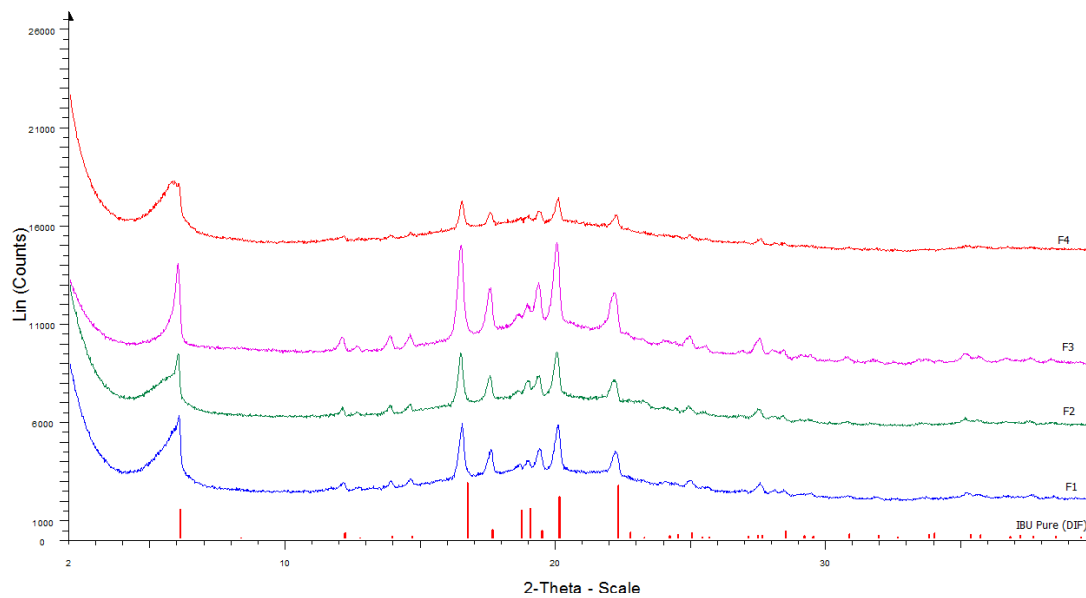
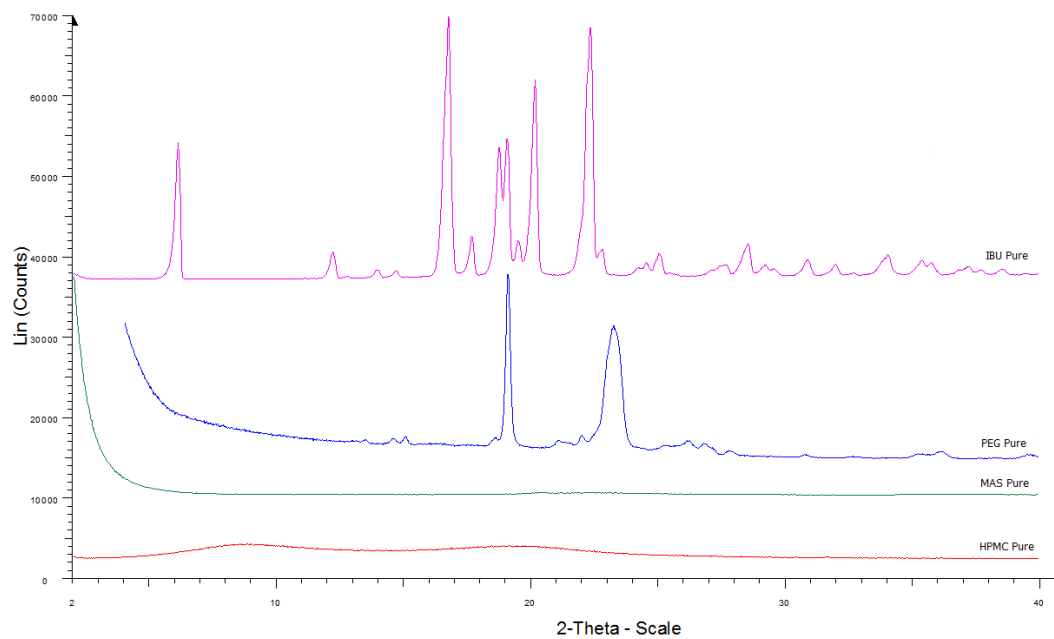
LOD Response Surface  
NEU/Polymer = 2.00



(c)



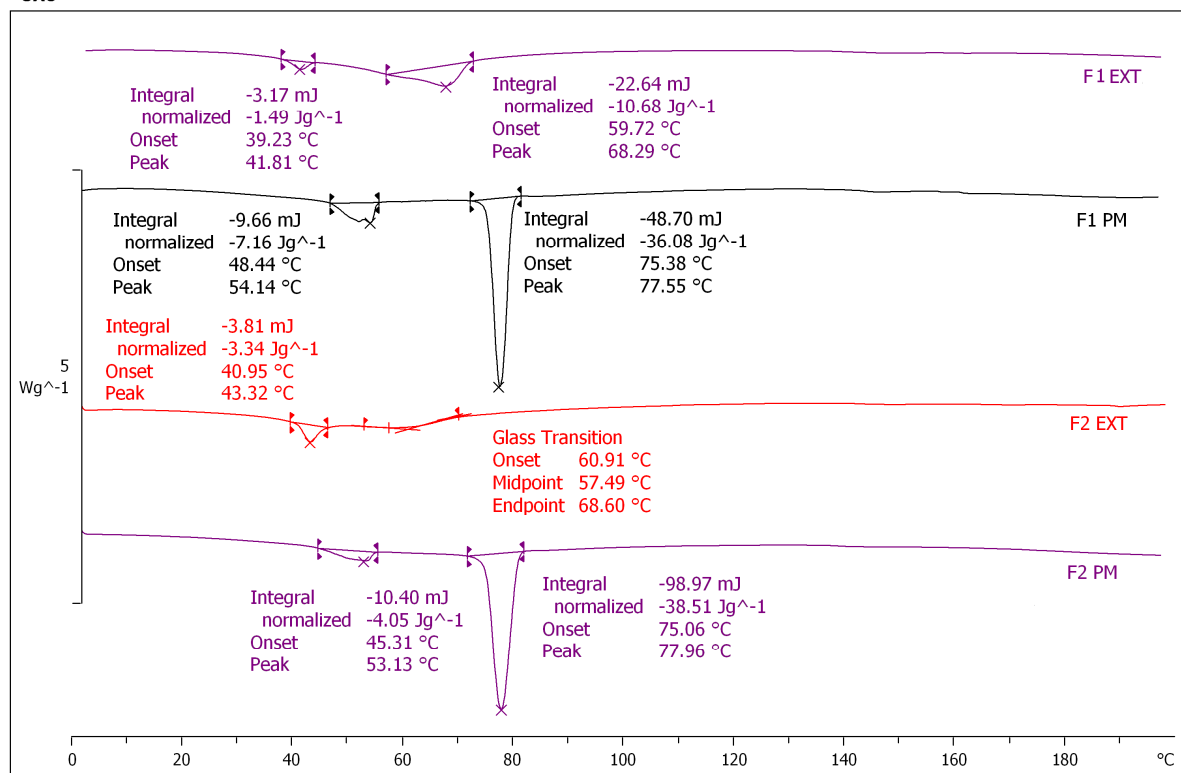








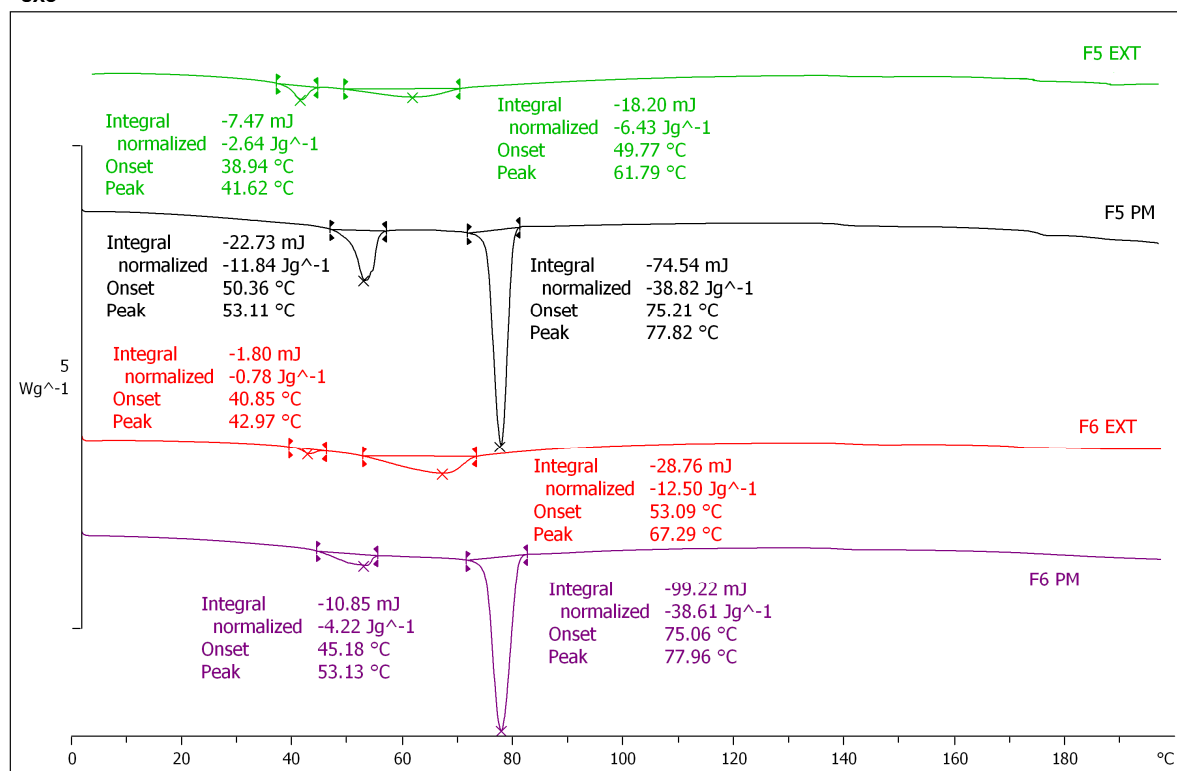
^exo



(i)

STAR<sup>®</sup> SW 10.00

^exo



(ii)

STAR<sup>®</sup> SW 10.00

